White Matter Alterations & Methionine Cycle Dysregulations in Mouse Models of Alzheimer's Disease

Lauren Kane[1], Alexandra Badea[2], Joan Wilson[3], Angela Everhart[3], Yi Qi[2], G. Allan Johnson, PhD[2] , Carol A. Colton, PhD[3]

[1]Trinity College of Arts and Sciences, Duke University, [2]Duke University Center for In-Vivo Microscopy, Durham, NC, and [3]Division of Neurology, Duke University Medical Center, Durham, NC,

Introduction

Alzheimer's disease (AD) is the only leading cause of death that is still on the rise[1]. In order to understand the pathology and progression of AD, our lab has developed a mouse model (APPSwDI/NOS2-/- ; CVN-AD) that mimics AD pathology. This mouse demonstrates the four major pathologies of AD – amyloid deposition, neuron loss, neurofibrillary tangle formation, and behavioral deficits. While AD is most strongly associated with plaques and tangles, myelin has been shown to be disrupted in patients with AD[2].

First, we studied changes in white matter tracts in the CVN-AD mouse model. If myelin is broken down, then the volume of these regions should be altered as well as the diffusion properties. Thus, through Diffusion Tensor Imaging (DTI), we examined changes in volume and changes in a diffusion parameter, known as fractional anisotropy (FA). FA represents the degree of directionality of water diffusion; a lower FA value likely reflects poor white matter myelination because diffusion is not well restricted by the myelin sheet.

Our second objective was to investigate a mechanism underlying the white matter alterations. We hypothesize that alterations in the methionine cycle contribute to the observed myelin breakdown in our AD models. The methionine cycle (shown below) is a well-known metabolic pathway that regulates gene expression through methylation, the additional of methyl groups.

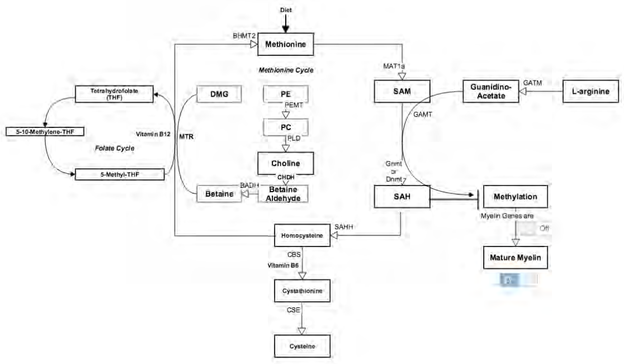

Patients with AD have altered levels of compounds instrumental in the methionine cycle[3]. Moreover, previous studies have shown an association between demyelination and methylation[4,5,6].

Thus, the **objectives** were **1)** to characterize the white matter of the CVN-AD models through diffusion-MRI and **2)** to identify gene expression changes in the methionine cycle in the CVN-AD mice across time.

Results: Atlas Based DTI

Volumes of CVN-AD brain regions are abnormal

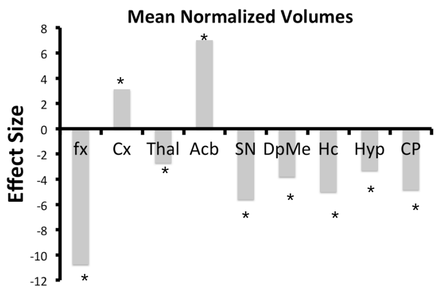

Among regions with significant differences in CVN-AD mice, the fornix (fx) is 10.8% smaller, and the hippocampus (Hc) is 5.0% smaller relative to the *mNos2*$^{-/-}$.

The effect sizes for the significant volume changes (p<0.05) are presented as a percent difference of the CVN-AD relative to the *mNos2*$^{-/-}$ controls.

CVN-AD mice show poor white matter integrity

Significant changes (p<0.05) in FA were observed in white matter regions in CVN-AD mice relative to mNos2-/- controls. For instance, the fornix (fx) has ~ a 10% lower FA (p<0.05). All of the significantly different brain regions have decreased FA in the AD models compared to *mNos2*$^{-/-}$ controls.

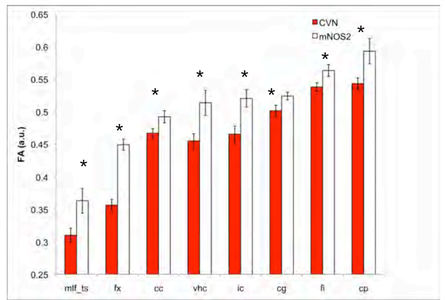

Results: Voxelwise DTI

Implicated brain regions are the same ones affected in AD patients!

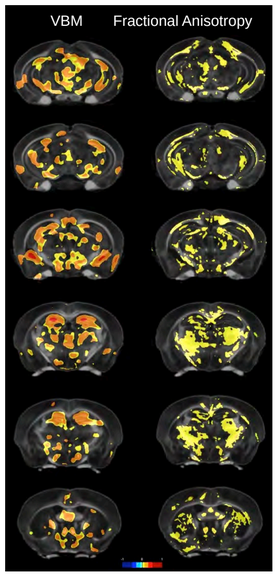

Effect size of uncorrected (significant p<0.05) volume (Voxel-based Morphometry) and FA in the CVN-AD relative to the *mNos2*$^{-/-}$ controls.

The CVN-AD mice show volumetric changes in the fornix and hippocampus.

Areas of decreased FA values in CVN-AD mice include the fornix, thalamus, corpus callosum, hippocampus, cortex.

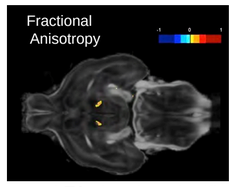

Corrected FA showing significant differences (p<0.05) in the fornix.

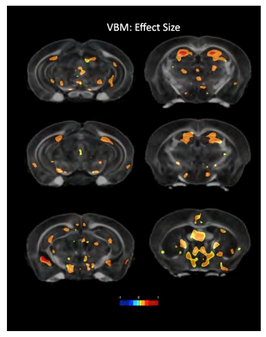

Effect size of corrected (significant p<0.05) volumes. The fornix and hippocampus are heavily implicated in CVN-AD mice.

Color bars legend: Warmer colors (red) represent larger changes in FA (smaller FA in CVN-AD), and local volumes (smaller in CVN-AD).

Results: Gene Expression Abnormalities

Different genes associated with the methionine cycle are dysregulated at different time points!

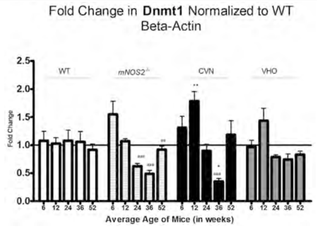

Dnmt1 is upregulated in 12 week and downregulated in 36 week CVN-AD mice

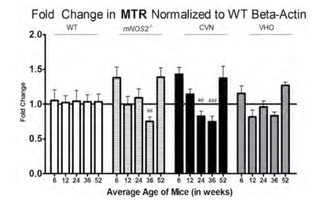

MTR is downregulated in 24 and 36 week CVN-AD mice.

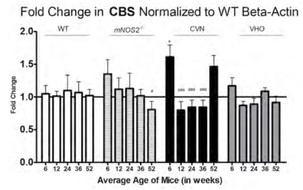

CBS is upregulated in 6 week CVN-AD mice

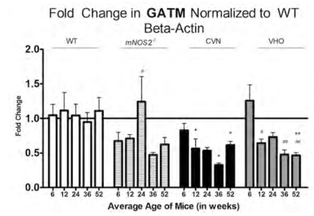

GATM is downregulated in 12, 36, and 52 week CVN-AD mice.

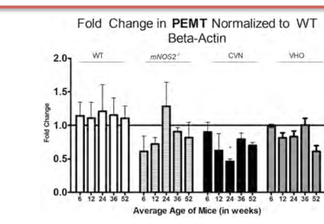

PEMT is downregulated in 24 week CVN-AD mice.

Data were analyzed using 2-way ANOVA (GraphPad Prism). Data points represent average fold change values ± SEM (N=5-8)
*** p<0.05, ** p<0.01, *** p<0.001 compared to WT mice of the same age.**
 # p<0.05, ## p<0.01, ### p<0.001 compared to 6-week mice of the same genotype.

Results: Summary of Dysregulations

Viewing the dysregulations in the context of the methionine cycle suggests…

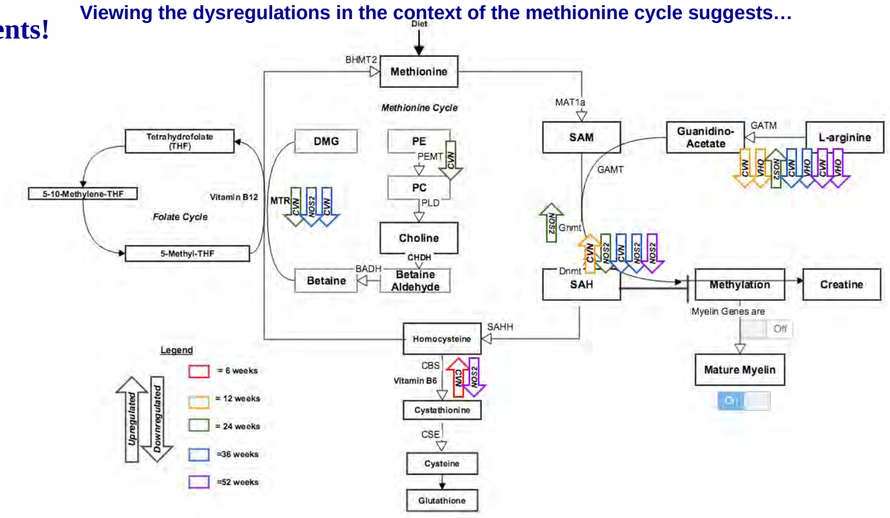

that many gene expression changes may code for enzymes to increase homocysteine levels and decrease methionine levels…. *suggesting impaired homocysteine metabolism?*

Conclusion

- Changes in volume and fractional anisotropy were observed in the brain of CVN-AD.
  - ✓ These changes indicate white matter atrophy in the CVN-AD model.
  - ✓ The areas of WM atrophy include well known AD circuitry, such as the hippocampus and fornix, validating the CVN-AD model.
- Dysregulations of genes involved in the methionine cycle were observed in the CVN-AD model .
  - ✓ This suggests that an epigenetic mechanism, mediated through improper methylation, may be critical to the development and progression of AD.
  - ✓ We speculate that the dysregulated genes may be coding for enzymes that increase homocysteine and divert methionine, altering methylation and contributing to pathology.

Methods

- **DTI**: Magnetic resonance histology of the mouse brain was done using a 9.4T magnet, using a diffusion tensor imaging protocol with 12 directions, TE=12ms, TR=100ms, b ≈ 1.5 × 10^3 s/mm^2 ; diffusion pulse width = 1.3 ms, separation = 6.4 ms, gradient amplitude = 1600 mT/m). A reference mouse brain atlas provided priors for automated segmentation of 38 regions[7]. We used advanced normalization tools[8] for image registration using the DWI and FA contrasts. SurfStat[9] was used for voxelwise statistics). Statistics were done using MATLAB and SurfStat.[9]
- **qPCR**: total RNA was extracted and homogenized. cDNA was produced using the cDNA High Capacity kit. Specific miRNA was reverse transcribed using the TaqMan MicroRNA Reverse Transcription Kit. The probes used: ß-actin, Dnmt1, Gnmt, MAT1a, PEMT, BHMT2, MTR, CBS, GAMT, GATM. Real-time PCR was performed using TaqMan Gene Expression assays and data were normalized to ß-actin. Average fold change values (RQ) were determined by 2-ΔΔCt method (All kits were from Life Technologies.)

References

[1] Alzheimer's Facts & Statistics. June 2014. BrightFocus Foundation.
[2]Gold B.T., Johnson N.F., Powell D.K. & Smith C.D. (2012). White matter integrity and vulnerability to Alzheimer's disease: preliminary findings and future directions. Biochim Biophys Acta. 1822(3):416-22.
[3]S. C. Marques, C. R. Oliveira, T. F. Outeiro, and C. M. Pereira, 'Alzheimer's Disease: The Quest to Understand Complexity', *J Alzheimers Dis*, 21 (2010), 373-83.
[4]S. Shen, J. Sandoval, V. A. Swiss, J. Li, J. Dupree, R. J. Franklin, and P. Casaccia-Bonnefil, 'Age-Dependent Epigenetic Control of Differentiation Inhibitors Is Critical for Remyelination Efficiency', *Nat Neurosci*, 11 (2008), 1024-34.
[5]R. Surtees, J. Leonard, and S. Austin, 'Association of Demyelination with Deficiency of Cerebrospinal-Fluid S-Adenosylmethionine in Inborn Errors of Methyl-Transfer Pathway', *Lancet*, 338 (1991), 1550-4.
[6]D. Ma, J. Huang, J. Huynh, P. Casaccia, C. Zhao, and R. Franklin, 'DNA Methylation in Cns Myelination and Remyelination', *Glia*, 59 (2011), S62-S62.
[7]Johnson, G. A., A. Badea, J. Brandenburg, G. Cofer, B. Fubara, S. Liu and J. Nissanov (2010). "Waxholm space: an image-based reference for coordinating mouse brain research." Neuroimage 53(2): 365-372.
[8]Avants, B. B., C. L. Epstein, M. Grossman and J. C. Gee (2008). "Symmetric diffeomorphic image registration with cross-correlation: evaluating automated labeling of elderly and neurodegenerative brain." Med Image Anal 12(1): 26-41.
[9]Worsley, K. J., J. E. Taylor, F. Carbonell, M. K. Chung, E. Duerden, B. Bernhardt, O. Lyttelton, M. Boucher and A. C. Evans (2009). "SurfStat: A Matlab toolbox for the statistical analysis of univariate and multivariate surface and volumetric data using linear mixed effects models and random field theory." Neuroimage 47, Supplement 1(0): S102.